

UMN-TH-1757/99
 TPI-MINN-99/23
 MADPH-99-1113
 hep-ph/9904393
 March 1999

MSSM Predictions for the Electric Dipole Moment of the ^{199}Hg Atom

Toby Falk¹

Department of Physics, University of Wisconsin, Madison, WI 53706, USA

Keith A. Olive² and Maxim Pospelov³

*Theoretical Physics Institute, School of Physics and Astronomy, University of Minnesota,
 Minneapolis, MN 55455, USA*

Radu Roiban⁴

*Institute for Theoretical Physics, State University of New York
 Stony Brook, N. Y. 11794-3840, USA*

Abstract

The Minimal Supersymmetric Standard Model can possess several CP-violating phases beyond the conventional Cabibo-Kobayashi-Maskawa phase. We calculate the contribution of these phases to T-violating nuclear forces. These forces induce a Schiff moment in the ^{199}Hg nucleus, which is strongly limited by experiments aimed at the detection of the electric dipole moment of the mercury atom. The result for d_{Hg} is found to be very sensitive to the CP-violating phases of the MSSM and the calculation carries far fewer QCD uncertainties than the corresponding calculation of the neutron EDM. In certain regions of the MSSM parameter space, the limit from the mercury EDM is stronger than previous constraints based on either the neutron or electron EDMs. We present combined constraints from the mercury and electron EDMs to limit both CP-violating phases of the MSSM. We also present limits in mSUGRA models with unified gaugino and scalar masses at the GUT scale.

¹falk@pheno.physics.wisc.edu

²olive@umn.edu

³pospelov@tpi1.hep.umn.edu

⁴roiban@insti.physics.sunysb.edu

1 Introduction

Despite the impressive success of the Standard Model, few are convinced that it is the final theory of particle interactions. For example, the supersymmetric modification of the Standard Model yields a very promising framework in which we are able to understand the stability of the electroweak scale. The Minimal Supersymmetric Standard Model (MSSM) provides a plethora of new phenomenological predictions which range from new charged and colored particles actively searched for in accelerators, to cold dark matter candidates, to new CP-violating phenomena such as the electric dipole moments of the neutron and electron which are generated if the additional CP-violating phases in the MSSM are non-zero. In this work, we study in detail the predictions of the MSSM for the electric dipole moment of the mercury atom and derive the constraints on the MSSM phases from the experimental limits on d_{Hg} .

The null experimental results for the electric dipole moments (EDMs) of the electron, neutron, heavy atoms and diatomic molecules [1, 2, 3, 4] can in general place very strong constraints on the CP-violating sector of a new theory and probe energy scales which are inaccessible for direct observations at colliders [5]. In general, the relevant contribution to the dipole moments at scales of ~ 1 GeV can be parameterized in terms of effective operators of different dimensions suppressed by corresponding powers of a high scale M where these operators were generated:

$$\mathcal{L}_{eff} = \sum_{n \geq 4} \frac{c_{ni}}{M^{n-4}} \mathcal{O}_i^{(n)}, \quad (1)$$

Here $\mathcal{O}_i^{(n)}$ are operators of dimension n , with its field content, Lorentz structures, etc., denoted by i . The fields relevant for the low-energy dynamics of interest are gluons, the three light quarks, the electron, and the electromagnetic field. This general form is independent of the particular construction of the new theory, and the details of a given model enter only through the values of the coefficients c_{ni}/M^{n-4} .

In the MSSM, the number of operators which can generate an EDM is considerably smaller than in the generic case. In fact, all four-fermion operators are numerically insignificant. They can be generated in the MSSM only with additional factor of order $(m_q/M_{SUSY})^2$ modulo possible nontrivial flavor structure of the soft-breaking sector. Here we assume the minimal scenario with flavor-blind breaking of supersymmetry and therefore we can safely drop all four-fermion CP-violating operators. Hence, the relevant part of the effective Lagrangian at the scale of 1 GeV contains the theta term, the three-gluon Weinberg operator, the EDMs of quarks and electron and the color EDMs (CEDMs) of quarks,

$$\begin{aligned} \mathcal{L}_{eff} = & \theta \frac{g_s^2}{32\pi^2} G_{\mu\nu}^a \tilde{G}_{\mu\nu}^a + w \frac{g_s^3}{6} f^{abc} G_{\mu\nu}^a \tilde{G}_{\nu\alpha}^b G_{\alpha\mu}^c \\ & + i \sum_{i=u,d,s} \frac{d_i}{2} \bar{q}_i F_{\mu\nu} \sigma_{\mu\nu} \gamma_5 q_i + i \sum_{i=u,d,s} \frac{\tilde{d}_i}{2} \bar{q}_i g_s t^a G_{\mu\nu}^a \sigma_{\mu\nu} \gamma_5 q_i + i \frac{\tilde{d}_e}{2} \bar{e} F_{\mu\nu} \sigma_{\mu\nu} \gamma_5 e. \end{aligned} \quad (2)$$

We will assume here that the PQ mechanism of θ -relaxation [6] eliminates $\theta \sim O(1)$ and sets θ to θ_{eff} at the minimum of the axion potential. When both the CEDMs and Weinberg

operator are absent, the value of θ_{eff} is exactly zero. However, nonzero w and \tilde{d}_i induce a linear term in the axion potential, and the effective value of θ is different from zero. This value leads to an additional contribution to the EDM of the neutron, usually ignored in the literature.

The coefficients in front of the operators in Eq. (2) can be calculated for any given model of CP-violation and then evolved down to the low-energy scale, using standard renormalization group techniques. In the MSSM, in particular, one can compute effective Lagrangian (2) for any given point in the supersymmetric parameter space. Then, to get the final predictions for EDMs, one has to take various matrix elements for these operators over hadronic, nuclear and atomic states [5, 7, 8, 9]. In most cases this is a source of major uncertainty, especially when hadronic physics is involved. The exception is the case of a paramagnetic atom, in which the EDM is generated by the electron EDM d_e , and where the effects of nuclear CP-odd moments induced by the rest of the operators in (2) can be safely neglected. The EDM of ^{205}Tl is extremely sensitive to d_e due to a very large relativistic enhancement factor $c \sim -600$, which relates the EDM of the atom with d_e , $d_{Tl} = cd_e$. The experimental bound on the EDM of the thallium atom [3], combined with good stability of atomic calculations (see [5] and references therein), leads to the following limit on the EDM of the electron:

$$d_e < 4 \cdot 10^{-27} e \cdot \text{cm}. \quad (3)$$

Therefore, the calculation of d_e in the MSSM gives the most reliable limits on CP-violating phases. It is clear, however, that the electron EDM limit alone cannot exclude the possibility of large CP-violating phases. This is because d_e , as any other coefficient in Eq. (2), is in general a function of *several* CP-violating phases, and mutual cancellations are possible. This is what happens, for example, in the MSSM with the minimal number of parameters in the soft-breaking sector (see recent works [10, 11]). In the MSSM, it is well known that there are two independent CP-violating phases, θ_μ and θ_A , associated with the supersymmetric Higgs mass parameter μ and the soft supersymmetry breaking trilinear parameter A . The calculation of the relevant one loop diagrams determines d_e as a function of these two phases. If the phases are small, d_e is simply a linear combination of θ_A and θ_μ . Therefore even a constraint as strong as that given in (3) leaves a band on the θ_A – θ_μ plane, along which a cancellation occurs and the phases are not constrained. In general, a second constraint could be expected to lift this degeneracy and place a strong constraint on both phases. It has been common to use the limit on the neutron EDM as this second constraint. Although there are large uncertainties in the calculation of the neutron EDM, as we argue below, when the limit on the neutron EDM is used, cancellations in the electron EDM occur in many of the same regions as cancellations in the neutron EDM. Therefore, one is led to the conclusion that large phases are still possible.

In what follows, we critically reexamine the reliability of the calculation of the EDM of the neutron in the MSSM. We demonstrate that this calculation is subject to very large hadronic uncertainties, which makes the extraction of the limits on CP-violating phases in MSSM tenuous. Instead, we propose that useful limits may be obtained from the limits on the EDM of the mercury atom. This arises from the T-odd nucleon-nucleon interaction

in the MSSM, induced mainly due to the CEDMs of light quarks. This interaction gives rise to an EDM of the mercury atom by inducing the Schiff moment of mercury nucleus. We demonstrate that the degree of QCD uncertainties related to this calculation is in fact smaller than in the case of d_n and that it is possible to calculate the T-odd nucleon-nucleon interaction as a function of the different MSSM phases. As an example, we proceed with the calculation of the EDM of the mercury atom in one specific point of the supersymmetric parameter space where all squark, gaugino masses, $|\mu|$ and $|A|$ parameters are set equal. This “pilot” calculation demonstrates the sensitivity of d_{Hg} to the CP-violating phases of MSSM. We find in this case that d_{Hg} provides somewhat better limits on CP-violating phases than d_e . We proceed further and combine mercury EDM and electron EDM constraints to exclude most of the parameter space on $\theta_A - \theta_\mu$ plane in this toy example. Finally, we consider more realistic constraints over the supersymmetric plane when supersymmetry breaking scalar and gaugino masses are unified at the GUT scale. In this case, we find that the limits on CP-violating phases obtained from d_{Hg} is no longer more restrictive than d_e , as the RG evolution of soft-breaking parameters makes squarks and gluino heavier than sleptons, charginos and neutralinos. The combined limits are still very powerful as the cancellation of different supersymmetric contributions typically occur in different regions of parameter space.

2 The Neutron EDM in the MSSM

Limits on the neutron EDM are commonly used to set constraints on new CP violating interactions. In particular, the upper limit to d_n is often used to limit the size of the CP-violating phases in the MSSM [12]. The current experimental limit on the EDM of the neutron is

$$d_n < 1.1 \cdot 10^{-25} e \cdot cm, \quad (4)$$

Indeed, the EDM of the neutron receives contribution from all operators listed above in Eq. (2) except d_e . However, there is a complication in using the neutron EDM as compared to the electron EDM, due to QCD uncertainties which make the extraction of the limits on CP-violating phases in the fundamental Lagrangian problematic. We demonstrate two aspects of this problem below.

The most straightforward contribution to the EDM of the neutron is due to the quark EDM operators. It is usually estimated using nonrelativistic SU(6) quark model. The result,

$$d_n = \frac{4}{3}d_d - \frac{1}{3}d_u, \quad (5)$$

can be compared, in fact, with the model calculations [13] and lattice simulations of light quark tensor charges in the nucleon [14]. The matrix elements for the tensor charges of the nucleon are defined by

$$\langle N | \bar{\psi}_q \sigma_{\mu\nu} \psi_q | N \rangle = \delta q \overline{N} \sigma_{\mu\nu} N, \quad (6)$$

whereas the axial charges are defined by

$$\langle N | \bar{\psi}_q \gamma_\mu \gamma_5 \psi_q | N \rangle = \Delta q \overline{N} \gamma_\mu \gamma_5 N \quad (7)$$

In the Naïve quark model, both Lorentz structures correspond to the spin of a nonrelativistic quark. In this case $\delta u = \Delta u = -1/3$, $\delta d = \Delta d = 4/3$, $\delta s = \Delta s = 0$, yielding eq. (5). Note that isospin symmetry gives us $(\Delta u)_n = (\Delta d)_p$, etc. However, as argued in [15], since it appears that the contribution to the nucleon spin from the strange quark (Δ_s) is non-vanishing [16], the naïve quark model may not be sufficient to describe the quark EDM contribution to the neutron EDM. While it is not the axial charges which need to be considered for the calculation of the neutron EDM, but rather the tensor charges, the departure of the axial charge values from their NQM values indicates that more realistic (non-NQM) values of the tensor charges (δq) must be used. According to calculations based on Lattice QCD [14], the tensorial charges of up and down quarks in the proton should be read as $\delta u \sim 0.8$ and $\delta d \sim -0.23$. This means that the naive nonrelativistic formula predicts the EDM of the neutron due to the quark EDMs to be 1.5-1.7 times larger than the lattice result. Slightly different values of $\delta u \sim 1.1$ and $\delta d \sim -0.4$ can be derived from the SU(3) chiral quark soliton model [13]. The tensor charge of the strange quark is found to be consistent with zero in both methods [13, 14]. This is due to the fact that the $\bar{s}\sigma_{\mu\nu}s$ operator is odd under charge conjugation which must result in the Zweig-type suppression of this matrix element over the neutron state. Even with the usual m_s/m_d enhancement of this operator, it is unlikely to be important. This does not exclude other possible CP-violating operators involving the s -quark, CEDM or generic four-fermion operators, as their contributions to the EDM of the neutron can be significant [7, 17]. Departures from the predictions of the non-relativistic quark model were recently considered in [18].

Unfortunately, the quantitative evaluation of the remaining contributions to the neutron EDM is complicated due to of our lack of knowledge about strong interaction dynamics at 1 GeV and below. Typically, one resorts to Naïve Dimensional Analysis (NDA) [19], formulated within the constituent quark framework. This method is, however, only an order of magnitude estimate to be used when other methods of calculation fail to produce an answer. When the problem of estimating d_N due to $\tilde{d}_{u,d}$ is considered, there are several possible answers in the literature:

$$d_N \simeq e0.7(\tilde{d}_u + \tilde{d}_d) \quad \text{Ref.[9]} \quad (8)$$

$$d_N \sim \frac{eg_s}{4\pi}(O(1)\tilde{d}_u + O(1)\tilde{d}_d) \quad \text{NDA, Ref.[20]} \quad (9)$$

We have chosen a normalization where g_s is included in the definition of the operator in (2) and correspondingly include an additional g_s in the estimate (9). The first result is based on a combination of chiral perturbation theory and QCD sum rules. The latter estimate is derived with the use of NDA¹. For a realistic choice of the strong coupling constant at the scale of 1 GeV, $g_s \sim \sqrt{0.5 \cdot 4\pi} = 2.5$, the overall numerical coefficient in eq. (9) is about 3.6 times smaller than in (8). Estimates based on NDA imply that for natural relations among coefficients $d_i/e \sim \tilde{d}_i$, the effects of color EDMs on the electric dipole moment of the neutron are negligible and the result can indeed be approximated by the linear combination of EDMS of quarks.

¹We note that the estimate in [21] is suppressed by an additional factor of $g_s/4\pi$.

In fact, it is possible to show that the CEDMs can lead to a substantially larger contribution to the neutron EDM than some of the predictions based on NDA. The easiest way to see that CEDMs can be numerically important is to calculate the effective θ -term induced by CEDMs in the presence of the PQ symmetry and then use the result for $d_N(\theta)$. This value, $\theta_{eff}(\tilde{d}_i)$ can be calculated within the current algebra approach, in a manner similar to the calculation of the vacuum topological susceptibility [22, 23, 24]. The dynamically induced theta term can be expressed in the following compact form:

$$\theta_{eff} = -\frac{m^2}{2} \left(\frac{\tilde{d}_u}{m_u} + \frac{\tilde{d}_d}{m_d} + \frac{\tilde{d}_s}{m_s} \right). \quad (10)$$

Here, m^2 is the ratio of the quark-gluon condensate to the quark condensate. It is known to good accuracy from QCD sum rules [25] that,

$$m^2 = \frac{\langle 0 | g\bar{q}(G\sigma)q | 0 \rangle}{\langle 0 | \bar{q}q | 0 \rangle} \simeq 0.8 \text{GeV}^2. \quad (11)$$

The accuracy of the estimate (10) is of order $m_{\pi,K}^2/m_{\eta'}^2$, which is acceptable for our purposes. If no interference with other terms is expected, then the expression (10) must be less than the current limit on θ , extracted from the same neutron EDM data. Using the fact that in the simplest variant of the MSSM, $\tilde{d}_d/m_d = \tilde{d}_s/m_s$, and assuming for a moment that this is the only contribution to the EDM of the neutron, one can obtain the following, quite stringent, level of sensitivity for the CEDM:

$$\tilde{d}_d < 10^{-25} \text{cm}. \quad (12)$$

This fact alone suggests that CEDMs may contribute significantly to the EDM of the neutron, typically at the level of the prediction (9) and an order of magnitude above NDA predictions. Remarkably, the main uncertainty in the limit (12) comes not from the calculation of $\theta(CEDM)$, but rather from the principal difficulties in calculating $d_N(\theta)$. In the standard approach [26], the chiral loop diagram is used to estimate $d_N(\theta)$. This loop is logarithmically divergent in the exact chiral limit and therefore is distinguished from the rest of the contributions. For realistic values of the parameters, however, this logarithm is not large and other contributions can be equally important. This makes the whole calculation problematic even in predicting the sign of the θ term contribution to d_N .

Besides $d_N(\theta(CEDM))$, one should also consider direct CEDM-induced contributions to the EDM of the neutron which can be computed within the same chiral loop approach [9]. Combining different contributions, we can symbolically write the result for the EDM of the neutron in the following form:

$$d_N \simeq 0.8d_d - 0.23d_u + e \left[\tilde{d}_u \left(c_1 \ln \frac{\Lambda}{m_\pi} + c_2 \right) + \tilde{d}_d \left(c_3 \ln \frac{\Lambda}{m_\pi} + c_4 \right) + \tilde{d}_s \left(c_5 \ln \frac{\Lambda}{m_K} + c_6 \right) \right]. \quad (13)$$

The coefficients c_1 , c_3 and c_5 were estimated in Ref. [9] to be $c_1 \ln(m_\rho/m_\pi) = c_3 \ln(m_\rho/m_\pi) \simeq 0.7$ and $c_5 \simeq 0.1$. The cutoff parameter Λ corresponds to scales where chiral perturbation

theory breaks down, that is, of order m_ρ . In the exact chiral limit, $m_\pi, m_K \rightarrow 0$, and the logarithmic terms dominate. In practice, however, the logarithmic terms are numerically not distinguished from the coefficients c_2, c_4 and c_6 , which are *a priori* comparable with c_1, c_3 and c_5 and are not calculable in this approach. It is clear then that these terms can change both the value and the signs of different contributions to d_N . Therefore, although in principle very important as an order of magnitude estimate, Eq. (13) fails to provide d_N as a known function of individual \tilde{d}_i -contributions and, ultimately, of different CP-violating phases.

As emphasized in Ref. [27], the NDA estimate of $d_n(\theta)$ essentially reproduces the calculation of Ref. [26]. The source of the disagreement in the case of $d_n(CEDMs)$ can be traced to the problem of estimating the CP-odd π^+pn -vertex, proportional to the matrix element $\langle p|\bar{u}g_s(G\sigma)d|n\rangle$. In Ref. [9] this matrix element was estimated to be -1.5 GeV^2 and is essentially proportional to the quark-gluon condensate parameter $m^2 \sim 0.8 \text{ GeV}^2$ (11). On the other hand, it can be shown that NDA suggests for this matrix element a value of order $4\pi f_\pi^2 \sim \text{GeV}^2/(4\pi)$, i.e. one order of magnitude smaller. This difference is related to the fact that the NDA assumes nonrelativistic quarks whose chromomagnetic interactions are suppressed, whereas QCD sum rules use more realistic descriptions of hadronic properties in terms of vacuum quark-gluonic condensates.

To summarize this discussion, the extraction of reliable limits on the CP-violating phases in the MSSM from the EDM of the neutron is difficult and uncertain. Even the best estimates of d_n based on the “chiral logarithm” approach [9], bear a large degree of uncertainty and cannot produce a precise prediction for d_n as a function of the CP-violating phases. Useful limits are still available from the electron EDM; however, the magnitude of the phases is not terribly constrained on this basis alone, due to cancellations in the various MSSM contributions to d_e . Fortunately, the EDM of the neutron is not the only source of information about CP-violation in the strongly-interacting sector. Limits on T-violating nuclear forces are provided by experiments aimed at the detection of the EDM of paramagnetic atoms, among which the EDM of ^{199}Hg atom is the most constraining. In what follows, we will discuss the constraints these limits provide, both alone and in conjunction with the electron EDM limits.

3 CP-violating nucleon-nucleon interaction in MSSM

The limits on T-odd nuclear forces extracted from the atomic experiments are in general very important for particle physics [5]. In the case of diamagnetic atoms, the most impressive limit is obtained for the EDM of ^{199}Hg [2]:

$$d_{Hg} < 9 \cdot 10^{-28} e \cdot \text{cm}. \quad (14)$$

The electric screening of the electric dipole moments of the atom’s constituents is violated by the finite size of the nucleus and can be conveniently expressed by the Schiff moment S , which parametrizes the effective interaction between the electron and nucleus of spin **I**,

$V_{eff} = -eS(\mathbf{I}\nabla)\delta(\mathbf{r})$ [5]. Atomic calculations derive the atomic EDM as a function of S and translate the experimental result (14) into the limit on the Schiff moment of the nucleus:

$$d_{Hg} = S \cdot 3.2 \cdot 10^{-18} \text{ fm}^{-2}$$

$$S < 2.8 \cdot 10^{-10} e \text{ fm}^3. \quad (15)$$

The Schiff moment of the nucleus can be induced either due to the Schiff moment of the valence nucleons or due to the breaking of time invariance in the nucleon-nucleon interaction, the latter being enhanced by the collective effects in the nucleus. The calculation of the Schiff moment of the nucleus, originating from various $\bar{N}N\bar{N}'i\gamma_5N'$ interactions was done in the single particle approximation with square-well and Woods-Saxon potentials [28]. The results show that the Schiff moment of mercury is primarily sensitive to the $\bar{p}p\bar{n}i\gamma_5n$ interaction. If we parameterize the coefficient in front of this interaction as $\xi G_F/\sqrt{2}$, the nuclear calculation [28] provides us with the following value for S :

$$S = -1.8 \cdot 10^{-7} \xi e \cdot \text{fm}^3. \quad (16)$$

Combined with Eq. (15), it gives the following constraint on ξ :

$$\xi < 1.9 \cdot 10^{-3}. \quad (17)$$

Questions concerning the calculation of the strength of $\bar{p}p\bar{n}i\gamma_5n$ interaction induced by different operators was considered in (2), [5, 8, 9]. The effective theta term, the Weinberg three-gluon operator and the CEDMs of quarks can generate this interaction. Numerically, the contributions provided by the CEDMs of up and down quarks are the most important and we concentrate our analysis on them, trying to incorporate the effect of \tilde{d}_s as well.

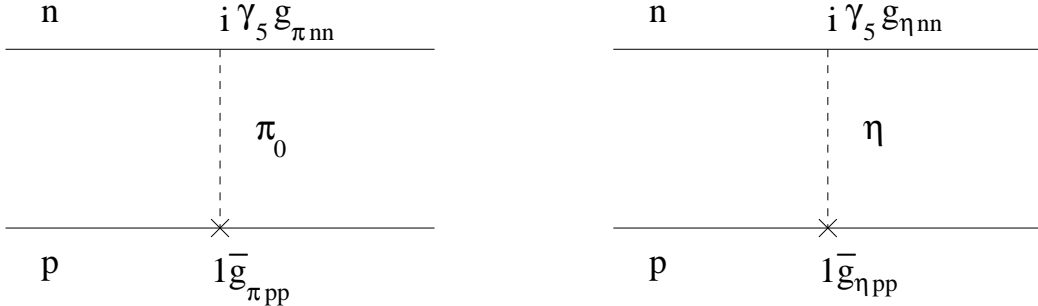


Figure 1: Pseudoscalar meson exchange diagrams, inducing $\bar{p}p\bar{n}i\gamma_5n$ interaction.

Following [8, 9], we approximate the T-violating nucleon-nucleon interaction by pseudoscalar exchange, as shown in Fig 1. In the limit of exact chiral symmetry this exchange has the power-like singularity m_π^{-2} , to be compared with the logarithmic singularity in the case of the EDM of the neutron. The CP violation resides in proton-meson vertex which can be calculated with QCD sum rules and current algebra techniques. The CP-conserving meson-neutron vertex is sufficiently well known from SU(3)-relations in baryon octet decay

amplitudes and from the axial charges of nucleons. If only \tilde{d}_u and \tilde{d}_d are present, the pion exchange dominates η exchange by a factor $m_\eta^2/m_\pi^2 \simeq 16$. In the MSSM, though, the strange quark CEDM is enhanced relative to that of the down quark by a factor m_s/m_d and η meson exchange is not *a priori* negligible. In the chiral approach, CP-violating vertices of interest can be reduced to the following set of matrix elements:

$$\begin{aligned}\bar{g}_{\pi pp} &= \frac{\tilde{d}_u + \tilde{d}_d}{4f_\pi} \left(\langle p | \bar{u}g_s(G\sigma)u - \bar{d}g_s(G\sigma)d | p \rangle \right) + \\ &\frac{\tilde{d}_u - \tilde{d}_d}{4f_\pi} \left(\langle p | \bar{u}g_s(G\sigma)u + \bar{d}g_s(G\sigma)d | p \rangle - m^2 \langle p | \bar{u}u + \bar{d}d | p \rangle \right) \\ \bar{g}_{\eta pp} &= -\frac{\tilde{d}_s}{\sqrt{3}f_\pi} \left(\langle p | \bar{s}g_s(G\sigma)s | p \rangle - m^2 \langle p | \bar{s}s | p \rangle \right)\end{aligned}\quad (18)$$

Here m^2 is the ratio of quark-gluon condensate to quark condensate introduced earlier in Eqs. (10) and (11). At this point our results are already slightly different from [7, 8, 29]. Namely, we have included additional contributions related to the fact that the octet combination of color EDM operators has the quantum numbers of the π^0 and η fields which can therefore be produced from the vacuum. π^0 , for example, can be “rescattered” on the nucleon with an amplitude proportional to $(m_d + m_u)\langle N | \bar{u}u + \bar{d}d | N \rangle$. As a result, the diagram shown in Fig. 2 is responsible for a contribution directly proportional to m^2 which is effectively of the same order as the direct contribution considered in [8, 9].

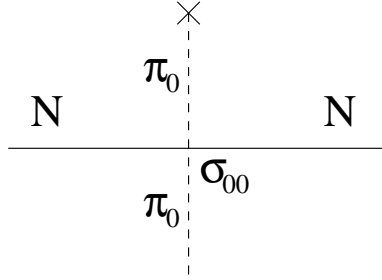


Figure 2: Additional contribution to the $\bar{g}_{\pi NN}$, proportional to the nucleon sigma term

Further calculation relies on QCD sum rules [22] and low-energy theorems in QCD. Matrix elements from $qg_s(G\sigma)q$ operators were evaluated in [7, 8, 29]:

$$\langle p | \bar{q}g_s(G\sigma)q | p \rangle \simeq \frac{5}{3}m^2 \langle p | \bar{q}q | p \rangle. \quad (19)$$

The matrix elements over the proton can be obtained from baryon mass splittings and pion-nucleon scattering data. Here we take the following values for the matrix elements of $\bar{q}q$ over the nucleon [29]:

$$\langle p | \bar{u}u | p \rangle \simeq 4.8; \quad \langle p | \bar{d}d | p \rangle \simeq 4.1; \quad \langle p | \bar{s}s | p \rangle \simeq 2.8 \quad (20)$$

These values of $\bar{q}q$ matrix elements correspond to the choice $m_u = 4.5$ MeV, $m_d = 9.5$ MeV and $m_s = 175$ MeV. The values of these matrix elements, together with the factorization formula (19), suggest that T-odd nucleon-nucleon forces are primarily sensitive to $\tilde{d}_u - \tilde{d}_d$ and insensitive to $\tilde{d}_u + \tilde{d}_d$, simply because the contribution to $\bar{g}_{\pi pp}$ proportional to $\tilde{d}_u + \tilde{d}_d$ in (18) is relatively suppressed by

$$\frac{\bar{g}_{\pi pp}(\tilde{d}_u + \tilde{d}_d)}{\bar{g}_{\pi pp}(\tilde{d}_u - \tilde{d}_d)} \simeq \frac{2\langle p|\bar{u}u - \bar{d}d|p\rangle}{\langle p|\bar{u}u + \bar{d}d|p\rangle} \sim 0.2 \quad (21)$$

In this sense, the contribution furnished by θ_{eff} is numerically insignificant because $\bar{g}_{\pi pp}$ generated by θ is also proportional to $\langle p|\bar{u}u - \bar{d}d|p\rangle$.

Thus, these simple considerations suggest that due to the numerical dominance of the triplet combination of color EDM operators, the final answer for ξ takes the following form:

$$\xi = G_F^{-1} \frac{3g_{\pi pp}m_0^2}{f_\pi m_\pi^2} (\tilde{d}_d - \tilde{d}_u - 0.012\tilde{d}_s), \quad (22)$$

We can see that the contribution of the strange quark CEDM is numerically suppressed, mainly due to the additional smallness of ηNN CP-conserving interaction as compared to $g_{\pi NN}$.

Combining equations (15), (16) and (22), we arrive at the following prediction for the EDM of the mercury atom:

$$d_{Hg} = -(\tilde{d}_d - \tilde{d}_u - 0.012\tilde{d}_s) \times 3.2 \cdot 10^{-2} e, \quad (23)$$

where the numerical coefficient $3.2 \cdot 10^{-2}$ corresponds to the choice of light quark masses given above. Using the experimental limits (14), we deduce the very strong constraint on the following combinations of the CEDMs of quarks:

$$|\tilde{d}_d - \tilde{d}_u - 0.012\tilde{d}_s| < 3.0 \cdot 10^{-26} cm. \quad (24)$$

It is important to note that the quark EDM operators cannot induce a large value for S . They do not induce the $\bar{n}i\gamma_f n\bar{p}p$ interaction, and their contribution to the Schiff moment of the nucleus is associated only with electric dipole moment of the external valence nucleon [5]. Current limits on d_{Hg} are only sensitive to quark EDMs larger than $10^{-24} e \cdot cm$ and thus these operators can be safely neglected. Similarly, the potential contribution from the three gluon operator $GG\tilde{G}$ to d_{Hg} are small. We rely here on the QCD sum rule estimates [30], showing no significant contribution from this operator to the T-odd nucleon-nucleon forces and thus to the EDM of mercury.

Finally, we would like to comment on the accuracy of the predictions (23) and (24), distinguishing between the error in the overall coefficients and the errors in the relative coefficients of \tilde{d}_i -proportional contributions. The uncertainties of the atomic calculations of $d_{Hg}(S)$ and nuclear calculations of $S(\xi)$ mostly affects the overall coefficients. Although the uncertainty in the overall coefficient can be significant [5], it is acceptable for our purpose as

it influences only the width of the allowed region in $\theta_\mu - \theta_A$ -plane. What is more important, however, is that the prediction of the relative coefficients in front of individual \tilde{d}_i in eqs.(23) and (24) can be done in a more reliable way and we estimate that the accuracy of keeping the triplet combination $\tilde{d}_d - \tilde{d}_u$ and neglecting $\tilde{d}_d + \tilde{d}_u$, eq. (21), is at the level of 20%. In effect, it makes the constraints imposed by d_{Hg} much more useful than those provided by d_n . Another advantage of the approach for calculating d_{Hg} and d_n , developed in refs. [8, 9, 5] and applied here, is that it reduces the error from the poor knowledge of the light quark masses. Indeed, even in the case of the naïve formula for the EDM of the neutron, $d_n \simeq (4d_d - d_u)/3$, the individual quark EDM contributions are proportional to $m_{u,d}$ which are known to 50%. In the present approach, the answer for ξ is ultimately proportional to a linear combination of $m_i \langle 0|\bar{q}q|0 \rangle$, which can be rewritten as $f_\pi^2 m_\pi^2$ times the function which depends only on the *ratio* of light quark masses, known to much better accuracy than the masses themselves.

4 The limits on the MSSM CP-violating phases

In previous work [11], limits on the neutron and electron dipole moments were used to constrain the two independent phases (of μ and A) in the MSSM assuming that all the terms in the Higgs potential and all gaugino masses are real and that all of the A -parameters are equal at the GUT scale and share a common phase. In absolute terms, the phases are not overly constrained, $\theta_\mu \lesssim 0.3$, for $\theta_A \simeq \pi/2$. The reason for the lax limits, are several cancellations in the various contributions to the EDMs. Furthermore, in some regions of parameter space, these cancellations occur simultaneously for the electron and neutron EDMs.

As we argued above, there are several reasons to suspect that the limit due to the neutron EDM must be treated with caution. Instead, we have argued that the limit coming from the EDM of Hg is the result of a “cleaner” calculation and carries fewer QCD uncertainties. In what follows, we will explore in detail the limits on the two phases using the constraint based on the EDM of ^{199}Hg (24) derived above. We will compare these constraints on the phases to that obtained from the electron EDM. As we will see, the cancellations in the EDMs do not always occur at the same points in parameter space. To demonstrate the importance of the mercury EDM limit, we first consider a SUSY model with a single mass scale. We then present general results which assume gaugino and sfermion mass universality at the GUT scale.

Following [31, 32], we analyze the limits on θ_A and θ_μ for different values of supersymmetric parameters. To demonstrate the sensitivity of the mercury EDM to a common scale of the supersymmetric masses with arbitrary and uncorrelated phases, we choose $m_{\tilde{f}} \simeq M_{\lambda_i} \simeq |\mu| \simeq |A_k|$ at the electroweak scale and take $\tan \beta = 2$. In Figures 3a and 3b, we show the sensitivity to the EDM of the mercury atom for the cases of $\sin \theta_A = 1$, $\sin \theta_\mu = 0$ and $\sin \theta_A = 0$, $\sin \theta_\mu = 1$. At this particular point of the supersymmetric parameter space all of the calculations are significantly simplified. When all soft-breaking parameters are

sufficiently heavy, close to the TeV scale, the chargino and gluino propagators can be simply expanded in v_1/M or v_2/M and only the zeroth and first order terms in the expansions need be kept. If needed, for lower values of gaugino masses, the results can be generalized to include all effects of mixing in the gluino and chargino sectors.

The calculation of the chromoelectric dipole moments of quarks in MSSM was done in the series of papers [20, 34, 35]. When the CEDMs of quarks are induced by θ_A , (as in Fig 3a), the result is dominated by gluino exchange, with very small corrections coming from λ_1 -exchange:

$$\begin{aligned}\tilde{d}_d &= -\eta \frac{m_d|A|\sin\theta_A}{16\pi^2 M^3} \left(\frac{5g_3^2}{18} - \frac{g_1^2}{108} \right) \\ \tilde{d}_u &= -\eta \frac{m_u|A|\sin\theta_A}{16\pi^2 M^3} \left(\frac{5g_3^2}{18} + \frac{g_1^2}{54} \right).\end{aligned}\quad (25)$$

Here η denotes the renormalization group factor which reflects the QCD evolution of the color EDM from the weak scale to 1 GeV. When the color EDM operator is defined as in eq. (2), its anomalous dimension is negative and small so that the overall renormalization of \tilde{d}_i is not important. The alternative definition of color EDM operator, frequently occurring in literature, is $\frac{1}{2}\tilde{d}'\bar{q}t^aG_{\mu\nu}^a\sigma_{\mu\nu}\gamma_5q$, where g_s is included in \tilde{d}' . Defined this way, this operator acquires a renormalization factor roughly proportional to $g_s(1\text{GeV})/g_s(M_Z) \simeq 2$ which is smaller than the value 3.3 quoted in [20]. This is because in Refs. [20, 35] a very large coupling constant at low energies, $\alpha_s \simeq 2$, is used. There is, however, an important numerical contribution to η which reflects the suppression of light quark masses at the high energy scale, $m_d(M_Z)/m_d(1\text{GeV})$. We choose to use low energy values for m_u and m_d , 4.5 and 9.5 MeV, and include the quark mass RG factor into η . For the scale M of order M_Z , η is numerically close to 0.35 and is mainly due to the suppression of the quark masses at the high energy scale. This suppression factor was omitted in Ref. [20] where $m_u(M_Z) = 8$ MeV is used.

Combining all numerical factors, we obtain the following value for the EDM of ^{199}Hg :

$$d_{Hg} = e \cdot 1.5 \cdot 10^{-2} \frac{5\alpha_3}{72\pi} \frac{(m_d - m_u - 0.012m_s)|A|\sin\theta_A}{M^3} \simeq 2 \cdot 10^{-27} \left(\frac{1\text{TeV}}{M} \right)^2 e \cdot cm, \quad (26)$$

where we simply take $|A| = M$. We see from Fig. 3a that the mercury EDM places a constraint on M , $M \gtrsim 1.5$ TeV.

In the other case, with $\sin\theta_A = 0$, $\sin\theta_\mu = 1$, we have to include λ_2 -higgsino and λ_1 -higgsino exchanges as well, so that the result for the CEDMs, (shown in Fig. 3b), is as follows:

$$\begin{aligned}\tilde{d}_d &= \eta \frac{m_d|\mu|\tan\beta\sin\theta_\mu}{16\pi^2 M^3} \left(\frac{5g_3^2}{18} + \frac{g_2^2}{8} + \frac{g_1^2}{216} \right) \\ \tilde{d}_u &= \eta \frac{m_u|\mu|\cot\beta\sin\theta_\mu}{16\pi^2 M^3} \left(\frac{5g_3^2}{18} + \frac{g_2^2}{8} + \frac{7g_1^2}{216} \right).\end{aligned}\quad (27)$$

As a result, the contribution of the up quark relative to that of the down quark is suppressed by $m_u/(m_d\tan^2\beta)$. Numerically, the gluino exchange diagram dominates again with less than

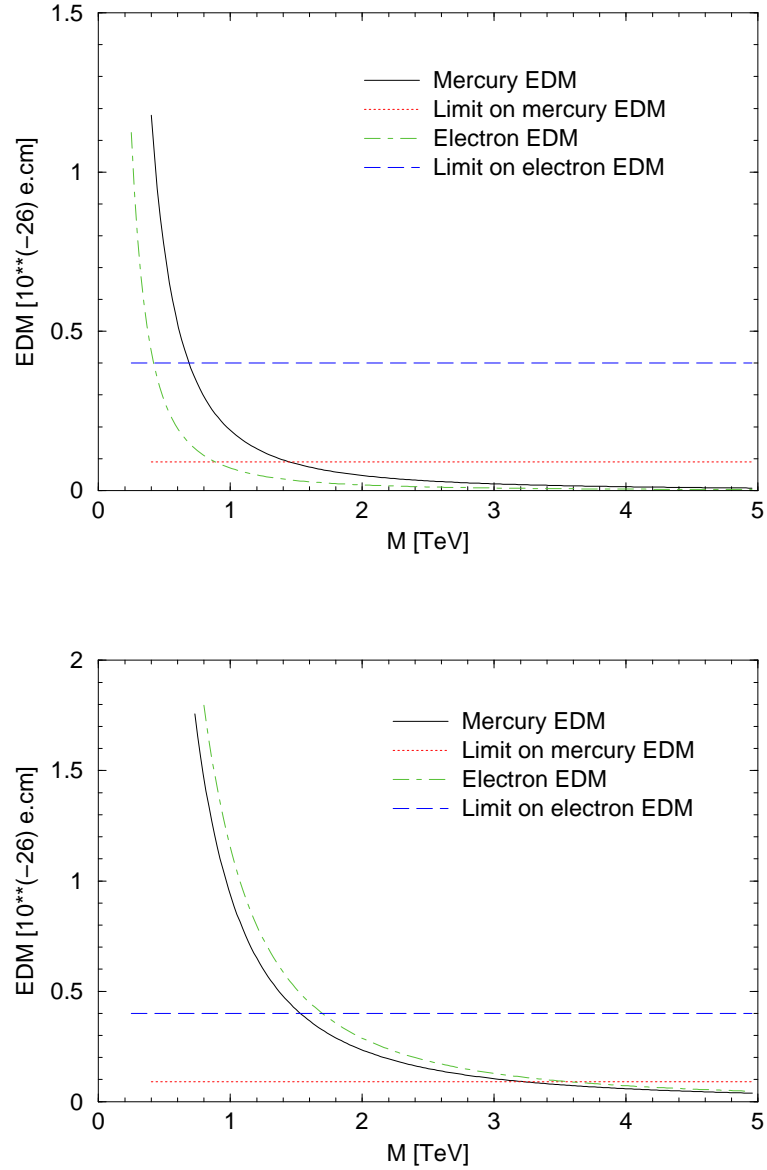


Figure 3: The sensitivity of the EDMs of mercury and electron to the scale of the soft-breaking parameters with a) maximal phase of A ($\theta_A = \pi/2, \theta_\mu = 0$), and b) maximal phase of μ ($\theta_A = 0, \theta_\mu = \pi/2$). We've taken $|\mu| = |A| = m_{\tilde{Q}} = m_{\tilde{U}} = m_{\tilde{D}} = M_{\lambda_i} \equiv M$. The horizontal line is the current experimental limit.

a 10% contribution coming from λ_2 -higgsino exchange. In this case, the limit is somewhat stronger giving, $M \gtrsim 3$ TeV.

As one can see, the EDM of mercury is sensitive to the scale of supersymmetric masses as high as 1.5-3 TeV. This can be compared with the sensitivity of the EDM of the electron, which we calculate at the same point of the supersymmetric parameter space, taking the slepton masses equal to the squark masses:

$$\begin{aligned} d_e &= \frac{m_e |A| \sin \theta_A}{16\pi^2 M^3} \frac{g_1^2}{12} \\ d_e &= \frac{m_e |\mu| \tan \beta \sin \theta_\mu}{16\pi^2 M^3} \left(\frac{5g_2^2}{24} + \frac{g_1^2}{24} \right). \end{aligned} \quad (28)$$

The limits based on the electron EDM, for the two cases considered, are weaker as can be seen from Fig. 3a and 3b where the limit on M is 0.4 and 1.7 TeV.

There is also the possibility of destructive interference between two contributions induced by the CP-violating phases. Again, we choose the supersymmetric parameters to be equal and fix them to be in the range from 250 – 750 GeV. Fig. 4a-4c show the combined exclusion plots. The two bands correspond to the parts of the parameter space where the mercury or electron (Tl) constraints are lifted by the cancellation of different supersymmetric contributions. The allowed area lies on the intersection of these two bands. We observe that the band corresponding to the mercury EDM constraint has a different slope than that of the electron EDM, mainly because d_{Hg} is by far more sensitive to θ_A . We observe that *both* phases are sufficiently constrained for the low values of M .

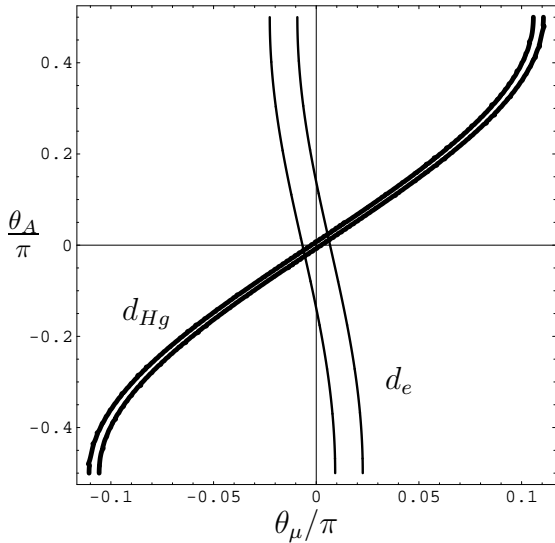


Fig. 4a: $M = 250$ GeV

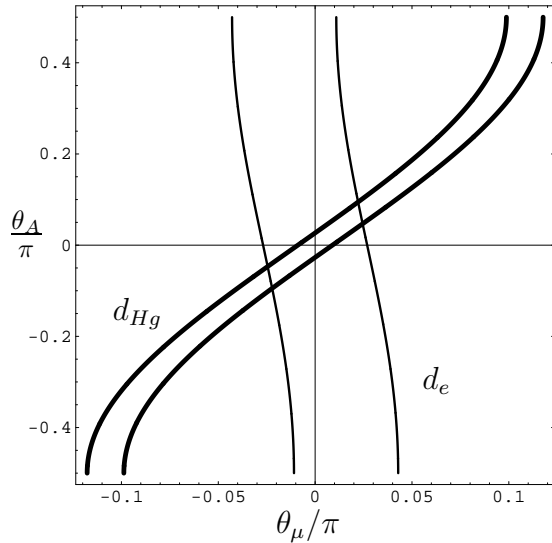


Fig. 4b: $M = 500$ GeV

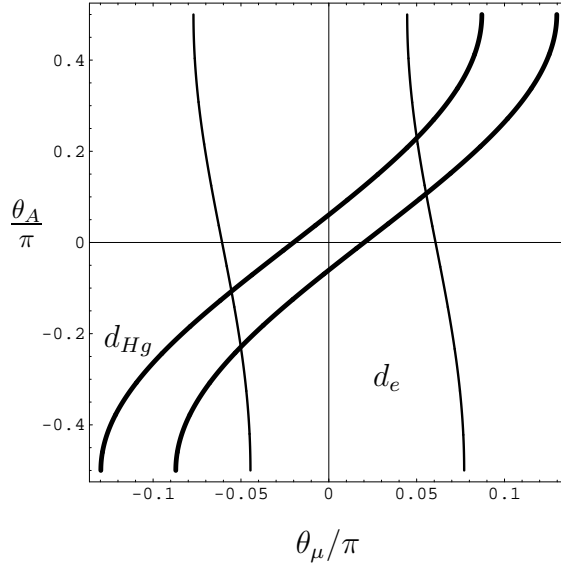


Fig. 4c: $M = 750$ GeV

Figure 4: Combined, d_{Hg} and d_e , constraints on the supersymmetric phases θ_A/π and θ_μ/π for different values of M . Allowed area is on the intersection of two bands.

5 EDMs in mSUGRA and Cosmological Constraints

We now consider the constraints on CP violating phases in mSUGRA-like models, i.e. models with unified gaugino and sfermion masses. We recall that to one loop, the phase of μ does not evolve with scale, but the phases of A_u , A_d and A_e must be run separately from the unification scale to low energies. We follow the analysis of [11, 32], but with two changes. First, we replace constraints from the neutron electric dipole moment with limits from the EDM of Hg, discussed above. Second, we include recent results on the effect of coannihilations of neutralinos with staus on the neutralino relic density [33]. The latter has the effect of weakening the cosmological upper bound on the gaugino masses. This is demonstrated in Fig. 5, where the light shading indicates the region of the $\{m_0, m_{1/2}\}$ plane which yields a neutralino relic abundance in the cosmologically preferred range $0.1 \leq \Omega_{\tilde{\chi}} h^2 \leq 0.3$. The upper limit of the light shaded region crosses below the line $m_{\tilde{\chi}} = m_{\tilde{\tau}_R}$ at $m_{1/2} \sim 1400$ GeV; for greater $m_{1/2}$, either the relic density violates the upper bound $\Omega_{\tilde{\chi}} h^2 \leq 0.3$ (which follows from a lower limit of 12 Gyr on the age of the universe) or the lightest supersymmetric particle is a stau, leading to an unacceptable abundance of charged dark matter. Here we've taken $\tan \beta = 2$, but the light shaded region is quite insensitive to $\tan \beta$ for the values of $\tan \beta$ we consider, as well as insensitive to the phase of μ [32]. For comparison, the dashed lines demarcate the inferred cosmologically preferred region if one ignores the effects of neutralino-slepton coannihilation. Whereas in [11], the constraint $\Omega_{\tilde{\chi}} h^2 \leq 0.3$ yielded an upper bound

of 450 GeV on $m_{1/2}$, we now have to consider larger values of $m_{1/2}$. However, we will see that this does not effect the upper bound on θ_μ .

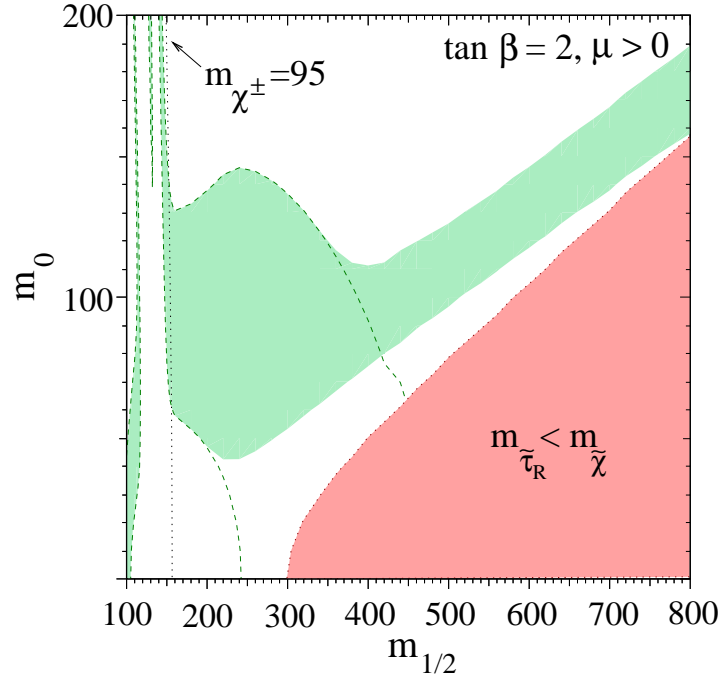


Figure 5: The light-shaded area is the cosmologically preferred region with $0.1 \leq \Omega_{\tilde{\chi}} h^2 \leq 0.3$. The dashed line shows the location of the cosmologically preferred region if one ignores the light sleptons. In the dark shaded region the LSP is the $\tilde{\tau}_R$, leading to an unacceptable abundance of charged dark matter. Also shown as a dotted line is the contour $m_{\chi^\pm} = 95$ GeV.

In contrast to the results of the previous section, we find that in mSUGRA-like models, constraints from the electron EDM are typically more restrictive than those from the EDM of Hg. This difference arises because in models with gaugino masses unified at the GUT scale, the gluino tends to be considerably heavier than the neutralino and charginos, and this suppresses the contribution to d_{Hg} from the quark chromoelectric dipole moments due to gluino exchange. We recall that cancellations between the chargino and neutralino exchange contributions to the electron EDM allow for large values of θ_μ [32, 35, 11]. A similar effect also applies in the case of the Hg EDM, where cancellations can occur between the gluino exchange and neutralino and chargino exchange contributions to the quark chromoelectric dipole moments. The power of combining the electron and Hg limits lies in the fact that for fixed θ_μ and θ_A , the cancellations in the electron and Hg dipole moments occur for different, and often non-overlapping, ranges in $m_{1/2}$. Thus the combined limits are stronger than either limit alone.

Following [32, 11], we compute the electron and Hg EDMs in mSUGRA as a function of θ_μ , θ_A and $m_{1/2}$ for fixed A_0 , m_0 and $\tan \beta$. In Fig. 6a-c we display the minimum value of $m_{1/2}$ required to bring both the electron and Hg EDMs below their experimental limits, for

$\tan \beta = 2$ and $m_0 = 130$ GeV. We exclude points which violate the current LEP2 chargino and slepton mass bounds [36]. The EDMs are computed on a 40x40 grid in $\{\theta_\mu, \theta_A\}$, and features smaller than the grid size are not significant. Although the dependence of the EDMs on $m_{1/2}$ is not monotonic, there is still a minimum value of $m_{1/2}$, due to cancellations, which is permitted. In the zone labeled “I”, $m_{1/2}^{\min} < 200$ GeV, while the zones labeled “II”, “III”, “IV” and “V” correspond to $200 \text{ GeV} < m_{1/2}^{\min} < 300$ GeV, $300 \text{ GeV} < m_{1/2}^{\min} < 450$ GeV, $450 \text{ GeV} < m_{1/2}^{\min} < 600$ GeV and $m_{1/2}^{\min} > 600$ GeV, respectively. Comparing with Fig. 5, we see that values of $m_{1/2}$ larger than about 600 GeV are cosmologically excluded for this value m_0 . Therefore, region V corresponds to an excluded region in the phase plane. Of course, for this value of $\tan \beta$, the current Higgs mass bound requires enormous sfermion masses $\gg 1$ TeV, which are cosmologically prohibited. We’ve chosen to plot our results for $\tan \beta = 2$ in order to compare to our previous results [32, 11]. Qualitatively similar conclusions apply for larger $\tan \beta$, which we summarize at the end of this section.

Figure 2 of Ref. [11] displays the corresponding contours to our Fig. 6a-c, but imposing only the constraint from the electron EDM². Note that in [11] we do not include a contour corresponding to $450 \text{ GeV} < m_{1/2}^{\min} < 600$ GeV, as this region would be cosmologically excluded in the absence of coannihilations of neutralinos with sleptons, whose effects were not included in [11]. The effect of including the Hg EDM bounds is particularly significant at large A_0 , where the cancellations are enhanced and the bounds on θ_μ are weakest. Here the widths of the allowed region in $m_{1/2}$ at fixed θ_A and θ_μ are narrowest, leaving less opportunity for overlap between the ranges allowed by the electron and Hg EDMs, respectively. Indeed, for $A_0 = 1.5$ TeV, the upper bound on θ_μ is reduced from $\sim 0.3\pi$, in the case of the electron EDM alone, to $\sim 0.18\pi$, combining the two constraints, and, further, the width of the region in θ_μ is considerably narrowed. The reduction in the bound on θ_μ is minimal for small A_0 , where the bounds on θ_μ are strongest. However, notice that the $m_{1/2}^{\min}$ at the largest allowed values of θ_μ is shifted from less than 200 GeV in the case of the electron EDM alone to between 200 and 300 GeV for the combined bound, in the case $A_0 = 300$ GeV. For $A_0 = 1$ TeV and 1.5 TeV, $m_{1/2}^{\min}$ lies above 300 GeV at the largest θ_μ .

We note that the larger values of $m_{1/2}$ which neutralino-slepton coannihilation permit do not increase the maximum θ_μ , for this value of m_0 . This is because, as we see from Fig. 6, the region of mutual cancellations happens to lie at lower $m_{1/2}$, between 300 and 400 GeV. The widths of the allowed regions in $m_{1/2}$ are typically between 50 and 80 GeV for the lightest shaded zones in Fig. 6b and 6c and greater than 80 GeV almost everywhere in Fig. 6a. Larger $m_{1/2}$ does, however, widen the allowed swath in θ_μ , by the region labeled “IV” in Fig. 6. It helps in particular at small θ_μ , where the electron EDM can be beaten down sufficiently by taking heavy gaugino masses, without resorting to cancellations between different contributions. At large $m_{1/2}$, the Hg EDM typically provides little constraint on θ_μ due to the heaviness of the gluinos. As m_0 is increased, the regions of cancellation shift, and the maximum value of θ_μ slowly decreases.

These effects are enhanced at larger m_0 and $m_{1/2}$, in the cosmologically allowed “trunk”

²In [11] we take $m_0 = 100$ GeV, rather than 130 GeV; however, taking $m_0 = 130$ GeV makes only a small change in the displayed contours and a slight reduction in the upper bound on θ_μ .

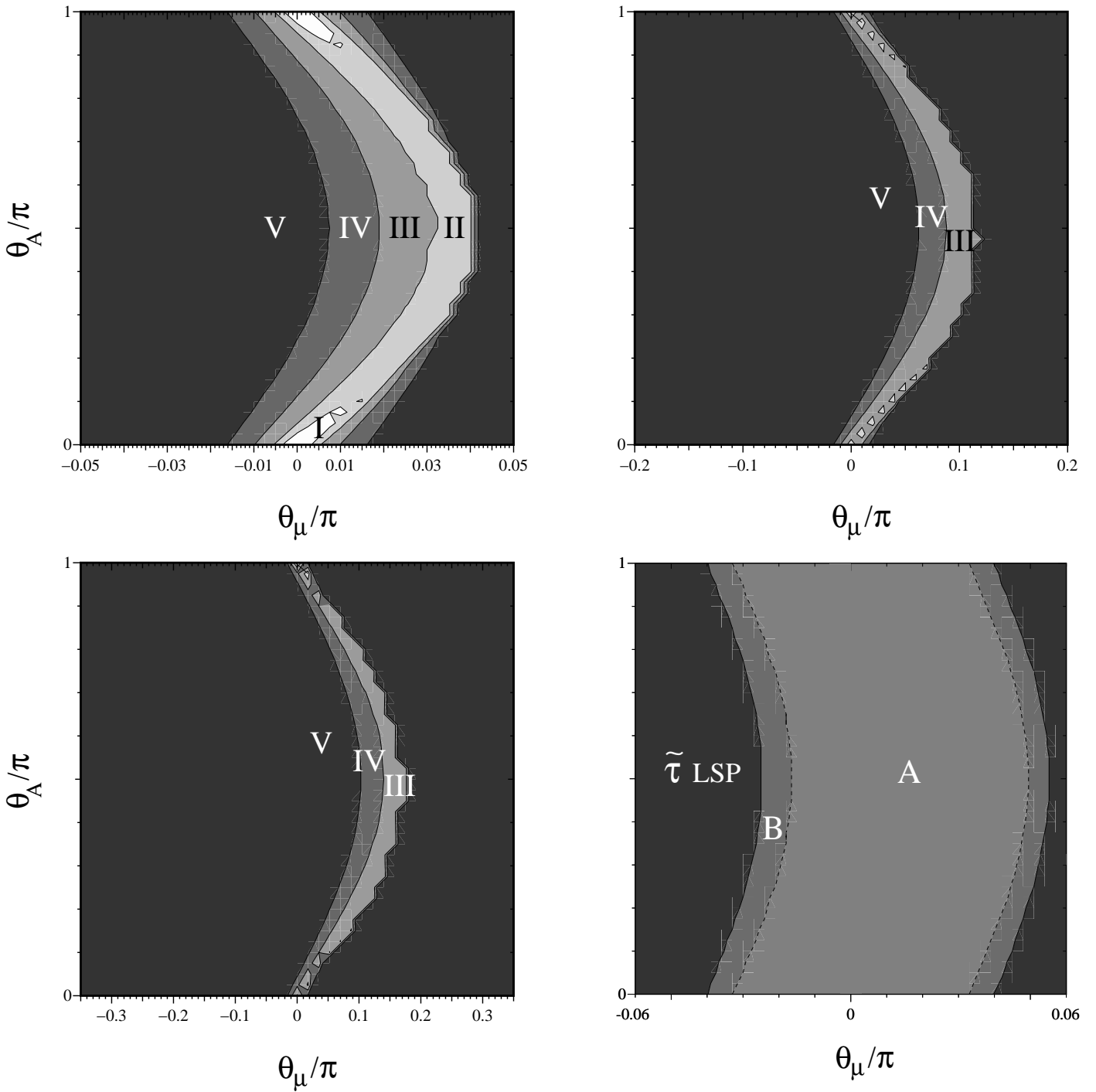


Figure 6: Contours of $m_{1/2}^{\min}$, the minimum $m_{1/2}$ required to bring both the electron and Hg EDMs below their respective experimental bounds, for $\tan\beta = 2, m_0 = 130 \text{ GeV}$, and a) $A_0 = 300 \text{ GeV}$, b) $A_0 = 1000 \text{ GeV}$ and c) $A_0 = 1500 \text{ GeV}$. The central light zone labeled “I” has $m_{1/2}^{\min} < 200 \text{ GeV}$, while the zones labeled “II”, “III”, and “IV” correspond to $200 \text{ GeV} < m_{1/2}^{\min} < 300 \text{ GeV}$, $300 \text{ GeV} < m_{1/2}^{\min} < 450 \text{ GeV}$, $450 \text{ GeV} < m_{1/2}^{\min} < 600 \text{ GeV}$ and $m_{1/2}^{\min} > 600 \text{ GeV}$, respectively. Zone V is therefore cosmologically excluded. Panel d) shows the allowed region in the “trunk” for $A_0 = 300 \text{ GeV}, m_0 = 200 \text{ GeV}$. The light shaded regions “A” and “B” are permitted, whereas the dark shaded region is cosmologically excluded (see the text).

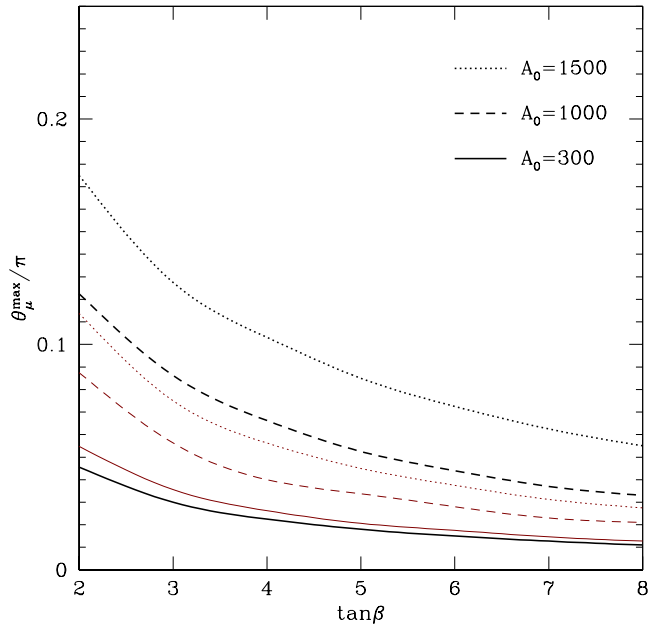


Figure 7: The maximum values of θ_μ allowed by cosmology and both the electron and Hg EDMs, as a function of $\tan\beta$, for $m_0 = 100$ GeV (thick lines) and $m_0 = 200$ GeV (thin lines) and for $A_0 = 300, 1000$ and 1500 GeV.

which lies on top of the $\tilde{\tau}_R$ LSP region (see Fig. 5). The allowed region narrows as m_0 increases, and the $\Omega_{\tilde{\chi}} h^2 = 0.3$ contour crosses the line $m_{\tilde{\tau}_R} = m_{\tilde{\chi}}$ and gives an upper bound on $m_{1/2}$ and m_0 at $m_{1/2} \sim 1400$ GeV, $m_0 \sim 300$ GeV. The trunk region yields much larger sparticle masses than are cosmologically permitted in the absence of coannihilations, and this can suppress the contributions to the electric dipole moments sufficiently so that significant cancellations between the various contributions are not necessary. For low A_0 , where the bounds on θ_μ are tightest, the bounds on θ_μ are somewhat relaxed in the trunk area. In Fig. 6d, we display the allowed region in the $\{\theta_\mu, \theta_A\}$ plane for $A_0 = 300$ GeV, $m_0 = 200$ GeV. For this value of m_0 , $m_{1/2}$ is cosmologically restricted to lie between 850 GeV and 950 GeV. In the light region labeled ‘‘A’’, the EDMs are below the experimental limits for all $850 \text{ GeV} \leq m_{1/2} \leq 950 \text{ GeV}$, while in the regions labeled ‘‘B’’, only part of this range of $m_{1/2}$ satisfies the EDM constraints. The dark regions at large $|\theta_\mu|$ require $m_{1/2} > 950$ GeV to satisfy the EDM bounds, and so these regions are cosmologically excluded, as they yield a stau LSP. The upper bound on θ_μ/π is relaxed to ~ 0.055 . Taking $m_{1/2}$ and m_0 at their maximal values allows θ_μ/π up to about 0.1.

For large A_0 , where θ_μ can take its maximal values, the bound on θ_μ does not weaken in the trunk region. As above, this is due to the fact that at larger θ_μ , cancellations are still required to bring the EDMs below their experimental limits, and the regions of cancellations occur at lower $m_{1/2}$. Even taking $m_{1/2}$ and m_0 at their largest cosmologically permitted

values does not allow for θ_μ larger than the bounds in Fig. 6b,c. Further, since the regions of low $m_{1/2}$ are cosmologically forbidden at large m_0 , the bounds on θ_μ at large A_0 actually decrease for large m_0 . Thus the presence of the coannihilation trunk region does not increase the overall combined cosmology/EDM bound on the phase θ_μ .

Lastly, we plot in Fig. 7 the maximum value of θ_μ allowed by the electron and Hg electric dipole moments and the upper limit on $\Omega_{\tilde{\chi}} h^2$, as a function of $\tan \beta$. The thick lines are for $m_0 = 100$ GeV, while the thin lines are for $m_0 = 200$ GeV and show the effect on the bounds described above as one moves into the trunk region.

6 Conclusions

We have shown that the calculation of the EDM of the neutron as the function of different MSSM phases is problematic due to large uncertainties related to the contributions of the color EDMs. This is in contrast to the electric dipole moment of the mercury atom, induced by the T-odd nucleon-nucleon interaction. In the chiral limit the coefficient ξ , characterizing the strength of T-odd forces has a power-like singularity $\sim m_\pi^{-2}$, whereas $d_N \sim \log m_\pi^2$ in the same chiral approach. It is apparent that the π^0 and η exchange diagrams dominate both parametrically and numerically and therefore yield a very good approximation to the magnitude of the T-odd interaction. The final result is proportional to $(\tilde{d}_d - \tilde{d}_u - 0.012\tilde{d}_s) \times 3.2 \cdot 10^{-2}e$ and can be further developed in terms of CP-violating phases of the MSSM.

There are two serious problems with the calculation of the T-odd nuclear forces due to the effective interaction (2) with the coefficients provided by the MSSM. First is the status of the factorization in Eq. (19), related with the low-energy theorem in 0^+ channel. Following Refs. [7, 8, 9], we have have taken $\langle p|\bar{q}g_s(G\sigma)q|p\rangle \simeq 1.3\text{GeV}^2\langle p|\bar{q}q|p\rangle$. We note that a designated sum rule calculation of this quantity and/or its simulation on lattice is highly desirable for it is the main source of uncertainties in the calculation of T-odd nuclear forces. The second potentially troublesome point is the effective negative sign between the \tilde{d}_d and \tilde{d}_s contributions. Although the numerical suppression in front of \tilde{d}_s is quite strong and d_d dominates, destructive interference is still possible in both cases, $\theta_A \neq 0$ and $\theta_\mu \neq 0$.

In this paper, we have considered first a very specific part of the supersymmetric parameter space, when all squark, slepton and gaugino masses were chosen to be equal. The theoretical prediction for d_{Hg} exhibits remarkable sensitivity to the scale of soft-breaking mass parameters as high as 1.5-3 TeV. When the scale is fixed below 1 TeV, d_{Hg} limits *both* phases. The constraints on the CP-violating supersymmetric phases, obtained in this way are the strongest constraints so far.

We have also considered the combined constraints from the Hg and electron EDMs in the mSUGRA, when all supersymmetry breaking gaugino masses, soft scalar masses, and soft trilinear terms are separately unified at the GUT scale. In this case, the sensitivity to the Hg EDM is weakened due to the relative size of the gluino mass. Nevertheless, the results are as strong or stronger (particularly when $|A|$ is large and the limits are weakest) than the combined results from d_e and d_N . The improvement in the limit is due to the fact that

cancellations among the contributions to the EDMs occur at slightly different regions of the SUSY parameter space.

7 Acknowledgments

M.P. would like to thank I.B. Khriplovich, A. Ritz, A.I. Vainshtein and A.R. Zhitnitsky for numerous important discussions. The work of M.P. and K.O. was supported in part by DOE grant DE-FG02-94ER-40823. The work of T.F. was supported in part by DOE grant DE-FG02-95ER-40896 and in part by the University of Wisconsin Research Committee with funds granted by the Wisconsin Alumni Research Foundation.

References

- [1] K.F. Smith *et al.*, Phys. Lett. **B234** (1990) 191; I.S. Altarev *et al.*, Phys. Lett. **B276** (1992) 242.
- [2] J.P. Jacobs *et al.*, Phys. Rev. Lett. **71** (1993) 3782.
- [3] E.D. Commins *et al.*, Phys. Rev. **A50** (1994) 2960.
- [4] D. Cho, K. Sangster and E. Hinds, Phys. Rev. Lett., **63** (1989) 2559.
- [5] I.B. Khriplovich and S.K. Lamoreaux, "*CP Violation Without Strangeness*", Springer, 1997.
- [6] R.D. Peccei and H. Quinn, Phys. Rev. Lett. **38** (1977) 1440.
- [7] V.M. Khatsimovsky, I.B. Khriplovich and A.R. Zhitnitsky, Z. Phys. **C36** (1987) 455.
- [8] V.M. Khatsimovsky, I.B. Khriplovich and A.S. Yelkhovsky, Ann. Phys. **186** (1988) 1.
- [9] V.M. Khatsimovsky and I.B. Khriplovich, Phys. Lett. **B296** (1994) 219.
- [10] T. Ibrahim and P. Nath, Phys. Rev. **D58** (1998) 111301; M. Brhlik, G. J. Good and G.L. Kane, hep-ph/9810457.
- [11] T. Falk and K.A. Olive, Phys. Lett. **B439** (1998) 71.
- [12] M. Dugan, B. Grinstein and L. Hall, Nucl. Phys. **B255**, 413 (1985); Y. Kizukuri & N. Oshimo, Phys. Rev. **D45** (1992) 1806; **D46** (1992) 3025.
- [13] H.-C. Kim, M.V. Polyakov and K. Goeke, Phys. Lett. **B387** (1996) 577.
- [14] S. Aoki *et al.*, Phys. Rev. **D56** (1997) 433.
- [15] J. Ellis and R. Flores, Phys. Lett. **B377** (1996) 83.

- [16] The EMC Collaboration, J. Ashman *et al.*, Phys. Lett. **B206** (1988) 364; for a review, see J. Ellis and M. Karliner, hep-ph/9601280.
- [17] C. Hamzaoui and M. Pospelov, hep-ph/9801363; C. Hamzaoui, M. Pospelov and R. Roiban, Phys. Rev. **D56** (1997) 4295.
- [18] A. Bartl, T. Gajdosik, W. Porod, P. Stockinger, and H. Stremnitzer, hep-ph/9903402
- [19] A. Manohar and H. Georgi, Nucl. Phys. **B234** (1984) 189.
- [20] R. Arnowitt, J.L. Lopez and D.V. Nanopoulos, Phys. Rev. **D42** (1990) 2423; R. Arnowitt, M.J. Duff and K.S. Stelle, Phys. Rev. **D43** (1991) 3085.
- [21] R. Barbieri, A. Romanino and A. Strumia, Phys. Lett. **B387** (1996) 310.
- [22] M.A. Shifman, A.I. Vainshtein and V.I. Zakharov, Nucl. Phys. **B166** (1980) 493.
- [23] I. Bigi and N.G. Uraltsev, Sov. Phys. JETP **100** (1991) 198.
- [24] M. Pospelov, Phys. Rev. **D58** (1998), 097703.
- [25] V.M. Belyaev and I.B. Ioffe, Sov. Phys. JETP **56** (1982) 493.
- [26] R. Crewther *et al.*, Phys. Lett. **B88** (1979) 123.
- [27] S. Weinberg, Phys. Rev. Lett. **63** (1989) 2333.
- [28] O.P. Sushkov, V.V. Flambaum and I.B. Khriplovich, Zh. Eksp. Theor. Fiz. **87** (1984) 1521 (Sov. Phys. JETP **60** (1984) 873).
- [29] A. Zhitnitsky, Phys. Rev. **D55** (1997) 3006.
- [30] V.M. Khatsimovsky, Yad.Fiz. **53** (1991) 548, [Sov.J.Nucl.Phys. **53** (1991)].
- [31] T. Falk, K.A. Olive and M. Srednicki, Phys.Lett. **B354** (1995) 99.
- [32] T. Falk and K. Olive, Phys. Lett. **B375** (1996) 196.
- [33] J. Ellis, T. Falk and K. Olive, Phys. Lett. **B444** (1998) 367.
- [34] I.B. Khriplovich and K.N. Zyablyuk, Phys. Lett. **B383** (1996) 429.
- [35] T. Ibrahim and P. Nath, Phys. Lett. **B418** (1998) 98; T. Ibrahim and P. Nath, Phys. Rev. **D57** (1998) 478.
- [36] R. Barate *et al.* [ALEPH Collaboration], Phys. Lett. **B433**, 176 (1998); ALEPH Collaboration, ALEPH 98-072; L3 Collaboration, L3 Note 2374.